

Published in final edited form as:

Circulation. 2007 January 23; 115(3): 345–352. doi:10.1161/CIRCULATIONAHA.106.633917.

Myocardial Ischemic Memory Imaging With Molecular Echocardiography

Flordeliza S. Villanueva, MD, Erxiong Lu, MD, PhD, Shivani Bowry, BS, Sevgi Kilic, PhD, Eric Tom, BS, Jianjun Wang, PhD, Joan Gretton, BS, John J. Pacella, MS, MD, and William R. Wagner, PhD

Cardiovascular Institute, Department of Medicine, University of Pittsburgh School of Medicine (F.S.V., E.L., S.B., S.K., J.W., J.G., J.J.P), and Department of Bioengineering (E.T., W.R.W.) and McGowan Institute for Regenerative Medicine (W.R.W.), University of Pittsburgh, Pittsburgh, Pa

Abstract

Background—Diagnosing acute coronary syndrome in patients presenting with chest discomfort is a challenge. Because acute myocardial ischemia/reperfusion is associated with endothelial upregulation of leukocyte adhesion molecules, which persist even after ischemia has resolved, we hypothesized that microbubbles designed to adhere to endothelial selectins would permit echocardiographic identification of recently ischemic myocardium.

Methods and Results—Lipid microbubbles (diameter, $3.3 \pm 1.7 \mu\text{m}$) were synthesized. The selectin ligand sialyl Lewis^x was conjugated to the microbubble surface (MB_{sLex}). Control bubbles (MB_{CTL}) bore surface Lewis^x or sialyl Lewis^c. Intravital microscopy of mouse cremaster muscle was performed after intravenous injection of MB_{sLex} (n=11) or MB_{CTL} (n=9) with or without prior intrascrotal tumor necrosis factor- α . There was greater adhesion of MB_{sLex} to inflamed versus noninflamed endothelium ($P=0.0081$). Rats (n=12) underwent 15 minutes of anterior descending coronary artery occlusion. After 30 minutes and 1 hour of reperfusion, high-mechanical-index nonlinear echocardiographic imaging was performed in which single frames were acquired at 3.5 and 4 minutes after intravenous injection of MB_{sLex} or MB_{CTL}. Video intensity at 4 minutes was subtracted from that at 3.5 minutes to derive target-specific acoustic signal. MB_{sLex} caused greater opacification in postischemic versus nonischemic myocardium at both time points ($P=0.002$). Immunostaining confirmed endothelial P-selectin expression in the ischemic bed.

Conclusions—Echocardiographic identification of recently ischemic myocardium is possible using ultrasound contrast agents targeted to selectins. This may offer a new approach to the more timely and precise diagnosis of acute coronary syndrome in patients presenting with chest pain of uncertain cardiac origin.

© 2007 American Heart Association, Inc.

Reprint requests to Flordeliza S. Villanueva, MD, University of Pittsburgh, Cardiovascular Institute, S568 Scaife Hall, 200 Lothrop St, Pittsburgh, PA 15213. villanuevafs@msx.upmc.edu.

Disclosures

None.

Keywords

cell adhesion molecules; contrast media; echocardiography; endothelium; imaging; ischemia

Chest discomfort accounts for 5 to 6 million patient visits to emergency departments in the United States annually.¹ The identification of acute cardiac ischemia in these patients constitutes one of the most difficult diagnostic challenges to emergency physicians. The diagnosis of an acute coronary syndrome (ACS) can be especially problematic in the absence of ECG abnormalities or elevated serum biomarkers indicating myocyte necrosis. The precise diagnosis of ACS is critical because the 2% to 7% of patients sent home inappropriately from emergency departments who are subsequently diagnosed with ACS represent a high-risk group, with a rate of fatal or potentially lethal complications of up to 26%.^{2,3} Conversely, to avoid a missed diagnosis of ACS, nearly 50% of patients presenting with chest pain are admitted,⁴ but ACS is confirmed in only 10% to 30% of these cases.⁵ Fifty percent of those admitted are subsequently found to have no significant coronary artery disease, amounting to a cost of \$1.7 million per life saved.^{4,6} This underscores the need to improve the triage and management of patients presenting with chest pain in whom unstable coronary artery disease may be the cause.

A hallmark of ischemia/reperfusion such as that which occurs during ACS is activation of the inflammatory cascade. This is characterized by sequential endothelial overexpression of leukocyte adhesion molecules that mediate leukocyte slowing, rolling, capture, and firm adhesion to the endothelium.⁷ Because adhesion molecules persist on the endothelial surface after ischemia has resolved, they represent a tissue “imprint” of the prior ischemic event. The adhesion molecule P-selectin is rapidly mobilized to the endothelial surface from preformed cytoplasmic stores within minutes of ischemia-reperfusion, followed by delayed, transcription-dependent endothelial overexpression of E-selectin, more P-selectin, intercellular adhesion molecule-1, and vascular cell adhesion molecule spanning the course of hours.⁸

Because these molecules are located on the luminal surface, we hypothesized that an intravascular probe that binds to selectins would detect the recent ischemic “memory” of myocardium and hence offer a new approach to the evaluation of patients presenting with recent or ongoing chest pain of possible coronary origin. Specifically, we tested the hypothesis that an acoustically active gas-filled microbubble bearing a selectin-specific ligand on its surface would bind to postischemic endothelium and that this property would enable echocardiographic detection of recent myocardial ischemia.

Methods

Surgical Preparation

The experimental protocols were approved by the Institutional Animal Care and Use Committee at the University of Pittsburgh.

Intravital Microscopy—Twenty adult CD-1 mice (25 to 30 g; Harlan Sprague Dawley, Inc, Indianapolis, Ind) were anesthetized (sodium pentobarbital, 0.1 mg IP). The right

jugular vein was cannulated for microbubble injection. The cremaster muscle was prepared for intravital microscopy as previously described.⁹

Ischemia Studies—Wistar rats (150 to 250 g, n=20; Harlan Sprague Dawley, Inc) were anesthetized (sodium pentobarbital, 0.35 mL IP), intubated, and mechanically ventilated. General anesthesia was maintained with 1.5% to 2.0% inhaled isoflurane. A 20-gauge catheter was placed in the internal jugular vein for microbubble injection. The carotid artery was cannulated with a 20-gauge fluid-filled catheter for intra-arterial pressure measurement. A lateral thoracotomy was performed, the pericardium was opened, and the anterior descending coronary artery was encircled with suture to permit reversible occlusion.

Microbubble Preparation

Phospholipid-based biotinylated ultrasound contrast microbubbles containing perfluorobutane gas were prepared.^{10–13} Fluorescent microbubbles were synthesized for intravital microscopy by adding rhodamine dihexadecanoyl phosphoethanolamine (Molecular Probes, Carlsbad, Calif). Microbubble diameter, measured by electrozone sensing (Multisizer-III, Beckman Coulter, Fullerton, Calif), was $3.3 \pm 1.7 \mu\text{m}$.

The microbubble targeting moiety was sialyl Lewis^x (sLe^x), the natural tetrasaccharide ligand for selectins.^{7,14} The control moieties, which lack significant selectin affinity, were Lewis-X (Le^x), which lacks the sialic acid residue, or 3'-sialyllactosamine (sLe^c), a defucosylated sLe^x. Biotinylated sLe^x, sLe^c, or Le^x (GlycoTech, Gaithersburg, Md) was conjugated to the microbubbles via multistep avidin/biotin bridging chemistry.^{10–13} Microbubbles conjugated to sLe^x are henceforth designated MB_{sLe^x}; microbubbles linked to sLe^c or Le^x are designated MB_{CTL}.

Intravital Microscopy

Intravital microscopy of mouse cremaster muscle was used to confirm microbubble adhesion using an inverted fluorescent microscope (Nikon TE200, Tokyo, Japan) connected to a digital camera (ORCA285, Hamamatsu, Hamamatsu City, Japan). Real-time images were captured (SimplePCI, Compix Inc, Sewickley, Pa) and analyzed offline by an observer blinded to experimental condition. Adhesion, defined as microbubble immobility lasting 30 seconds,¹⁵ was quantified in venules at 7 minutes after microbubble injection in 20 random fields. Centerline blood velocities were measured with a dual-slit photodiode and converted to mean blood velocities by multiplying by a factor of 0.625.¹⁶ Wall shear rate (γ_w) was calculated using the following equation:

$$\gamma_w = 2.12 \left(\frac{8V_b}{d} \right),$$

where V_b is mean red cell velocity, d is vessel diameter, and 2.12 is a correction factor for the velocity profile.¹⁷

Myocardial Contrast Echocardiography

Myocardial contrast echocardiography (MCE) was performed with an ultrasound system using a nonlinear multipulse imaging scheme (8 MHz, Contrast Pulse Sequencing, Sequoia, Siemens Corp, Mountain View, Calif). Images were acquired in open-chest animals at a mechanical index of 1.5, which disrupts microbubbles.¹⁸ Probe position, dynamic range, gain settings, and focus were initially optimized and maintained. ECG-triggered end-systolic images were acquired at baseline (before injection) and 3.5 and 4 minutes after microbubble injection. Average pixel video intensity (gray level) in digitized images was measured in 2 regions of interest corresponding each to the ischemic and nonischemic beds. Video intensity at 4 minutes (background signal from residual circulating microbubbles) was subtracted from video intensity at 3.5 minutes (signal from adhered microbubbles plus circulating microbubbles) to yield the signal attributable to specific adhesion.^{11,12,15,19} Additionally, the 4-minute frame was digitally subtracted from the 3.5-minute frame, and the resulting image was color-coded using a map wherein shades of red, progressing to orange, yellow, and white, represented increasing contrast enhancement.^{11,12}

The risk area during occlusion and region of contrast enhancement during MB_{sLex} injection were planimetered and expressed as a percent of the area of the short-axis left ventricular slice.

Histological Studies

Postmortem, the heart was excised and cross-sectioned into 3 short-axis slices. The slice corresponding to the imaging plane was stained with triphenyl tetrazolium chloride to delineate infarction. Another slice immediately basal or apical to the triphenyl tetrazolium chloride-stained slice was frozen in liquid nitrogen, cryosectioned, and stained using primary antibodies against CD31, P-selectin, E-selectin, and intercellular adhesion molecule-1 for multicolor fluorescent immunohistochemistry (Santa Cruz Biotechnology, Inc, Santa Cruz, Calif).

Experimental Protocols

Intravital Microscopy—Mice were studied under either basal (n=10) or inflammatory (n=10) conditions in which tumor necrosis factor- α (0.5 μ g, EMD Biosciences, San Diego, Calif) was injected into the scrotum 5 hours before surgical preparation. Each mouse received either 1 intravenous injection of 5×10^7 MB_{sLex} (n=11) or MB_{CTL} (Le^x conjugated; n=9) in 200 μ L phosphate-buffered saline, followed by a 200- μ L saline flush. Each animal was randomly assigned as either inflammatory or noninflammatory and then randomly assigned to receive 1 of the 2 microbubble species. At the end of the experiment, mice were euthanized with a pentobarbital overdose.

Targeted Echocardiographic Imaging During Reperfusion—A rat model of myocardial ischemia-reperfusion (n=18) was used.²⁰ The anterior descending coronary artery was occluded for 15 minutes (n=14). Twenty minutes after reperfusion, 5×10^7 nontargeted microbubbles (biotinylated lipid microbubbles) in 200 μ L saline were intravenously injected to confirm successful reperfusion, to optimize imaging settings, and to verify myocardial contrast disappearance by 3.5 minutes after injection. Thirty minutes

after reperfusion, 5×10^6 MB_{sLex} or MB_{CTL} (sLe^c conjugated) in 200 μ L saline were intravenously injected, and MCE imaging was performed. Imaging was repeated ≈ 1 hour after reperfusion. Each rat received 1 injection each of MB_{sLex} and MB_{CTL}, with the microbubble type making up the first injection alternating between consecutive rats to minimize potential systematic differences arising from any time-related variations in selectin expression. The anterior descending coronary was reoccluded antemortem during nontargeted MCE to delineate the risk area. All MCE imaging was completed by 2 hours after reperfusion. The rats were euthanized with pentobarbital overdose, and the heart was excised.

To explore whether ischemic memory could be elicited by shorter durations of ischemia, an additional 4 rats underwent only 10 minutes of coronary artery occlusion followed by MCE imaging 1 hour after reperfusion. Two additional rats underwent 15 minutes of occlusion and were euthanized at 45 minutes of reflow solely for collection of immunohistological data.

Statistical Analysis

Data are expressed as mean \pm SD. Nonparametric comparisons among experimental conditions during intravital microscopy were performed with the Kruskal-Wallis test, and preplanned post hoc comparisons were conducted using the Wilcoxon-Mann-Whitney test. Nonparametric within-group comparisons were performed with the Wilcoxon signed rank-sum test for paired samples. The relationship between size of the risk area and size of the region of postischemic contrast enhancement was assessed using linear regression analysis. Significance was defined as $P < 0.05$ for the Kruskal-Wallis test (2 tailed). Bonferroni criteria were used to correct for multiple comparisons during post hoc testing; significance was defined as $P < 0.025$ (2 tailed).

The authors had full access to the data and take full responsibility for the integrity of the data. All authors have read and agree to the manuscript as written.

Results

Intravital Microscopy

Figure 1 illustrates micrographs of venules within cremaster muscle; the bright-field image is shown on the left and the corresponding fluorescent field of view is shown on the right side of each panel. In noninflamed muscle, there was minimal venular adhesion of either MB_{CTL} (Figure 1A) or MB_{sLex} (Figure 1B). Within inflamed muscle, there was scant venular adhesion of MB_{CTL} (Figure 1C), whereas there was more adhesion of MB_{sLex} (Figure 1D).

Microbubble adhesion varied among the 4 experimental groups (Kruskal-Wallis test χ^2 , 11.39; $P = 0.0098$) (Figure 2). Adhesion of MB_{sLex} to inflamed venules (8 ± 5 bubbles per field) was higher than adhesion to noninflamed venules (1 ± 1 bubbles per field; $P = 0.0081$). Among the inflamed mice, there was a trend toward greater adhesion of MB_{sLex} (8 ± 5 bubbles per field) compared with MB_{CTL} (3 ± 2 bubbles per field; $P = 0.07$). Venular wall shear rates were comparable across all 4 experimental conditions.

Targeted Echocardiographic Imaging During Reperfusion

All rats in the 10-minute occlusion group ($n=4$) survived. Of the 14 rats undergoing 15 minutes of occlusion, 2 died of ventricular fibrillation immediately after reperfusion. Image data were collected for the remaining 12 rats in this group. Because of technical issues, targeted images at both 30 and 60 minutes could not be acquired in all 12 rats; 30-minute data were acquired in 10 rats, and 60-minute images were acquired in 11 rats.

Risk area size in the entire group was $41\pm 11\%$ of the left ventricular short-axis slice. Infarct size was $13\pm 15\%$ of the short-axis slice of the left ventricle, with 10 rats having $<15\%$ infarction (including 6 with 0% infarction).

Background-subtracted color-coded MCE images at 30 minutes after reperfusion in 1 rat undergoing 15 minutes of occlusion are shown in Figure 3. During occlusion and injection of plain microbubbles, there was a risk area involving the anterior septum and anterior wall (Figure 3A). After reperfusion, nontargeted MCE showed homogeneous myocardial enhancement, indicating restoration of blood flow (Figure 3B). Triphenyl tetrazolium chloride staining confirmed the absence of infarction (Figure 3C). The MCE images representing subtraction of the 4-minute frame from the 3.5-minute frame after injection of MB_{sLex} or MB_{CTL} are shown in Figure 3D and 3E, respectively. There was persistent contrast enhancement by MB_{sLex} (Figure 3D) in the myocardial region corresponding to the previously ischemic area (Figure 3A). There was minimal myocardial opacification from MB_{CTL} , and because tissue background is minimized by the nonlinear imaging platform of the ultrasound machine, the MCE image was nearly black (Figure 3E).

There were significant differences in video intensity as a function of microbubble type and ischemia status at 30 minutes after reperfusion ($n=10$) (Figure 4). After MB_{sLex} injection, video intensity in the postischemic bed (15 ± 7) was higher compared with nonischemic myocardium (2 ± 3 ; $P=0.002$). In the postischemic bed, video intensity was higher after MB_{sLex} injection (15 ± 7) than after MB_{CTL} (6 ± 6 ; $P=0.002$).

In 11 of the 12 rats surviving the 15-minute occlusion protocol, targeted images were collected at 1 hour (range, 50 to 93 minutes) after reperfusion. After MB_{sLex} injection, video intensity in the postischemic bed (13 ± 8) was higher compared with that in nonischemic myocardium (2 ± 3 ; $P=0.001$). In the postischemic bed, video intensity was higher after injection of MB_{sLex} (13 ± 8) than after injection of MB_{CTL} (5 ± 6 ; $P=0.001$). Paired analyses of the video intensity data in the 9 rats with complete 30-minute and 1-hour reperfusion images revealed no statistically significant differences in video intensity measurements between the 2 reperfusion time points.

In the 4 rats undergoing only 10 minutes of ischemia and targeted imaging at 1 hour after reflow, video intensity in the ischemic and nonischemic beds after MB_{sLex} injection was 9 ± 5 and 1 ± 1 , respectively; in the ischemic bed, video intensity after MB_{CTL} injection was 2 ± 2 .

A significant linear relationship was found between risk area size and the size of the region of persistent contrast enhancement by MB_{sLex} for both the 30-minute reflow images

($r=0.95$, $P<0.0002$) (Figure 5) and the 60-minute reflow images ($r=0.77$, $P<0.0009$) in rats undergoing the 15-minute occlusion.

Myocardial immunostaining (Figure 6) demonstrated strong microvascular P-selectin expression in the ischemic bed (Figure 6A), which was not seen in the nonischemic bed (Figure 6E). Staining for adhesion molecules intercellular adhesion molecule-1 and E-selectin, as well as staining with nonspecific immunoglobulin G as the primary antibody, demonstrated no significant uptake in either ischemic (Figure 6B through 6D) or nonischemic tissue (Figure 6F through 6H).

Discussion

The main finding of the present study is that postischemic myocardium can be identified ultrasonically with micro-bubbles targeted to adhesion molecules expressed acutely during ischemia/reperfusion. Specifically, we demonstrated that an ultrasound contrast agent targeted to the selectin family of adhesion molecules adheres to inflammatory endothelium. Furthermore, we showed that selectin-targeted microbubbles permit echocardiographic identification, localization, and spatial quantification of the postischemic region.

Challenges in the Diagnosis of ACS

Routine clinical tests for the diagnosis of ACS have limitations. In 1 study, 38% of patients ultimately diagnosed as having unstable angina had normal or nondiagnostic ECGs.²¹ The sensitivity of cardiac serum biomarkers for acute infarction is low early after symptom onset and similarly low for detecting ischemic chest pain in the absence of necrosis.²² Although echocardiographic wall motion analysis can be helpful,²³ its specificity is low when remote events such as stable prior infarction coexist. MCE has shown promise,²⁴ but perfusion may appear normal if chest pain has resolved, and the presence of a perfusion defect cannot distinguish between active ischemia (the diagnostic goal) and remote infarction.

Single-photon emission computed tomography perfusion imaging may improve the triage of patients with chest pain^{5,25} but is limited by false negatives if ischemia has resolved before isotope injection and by false positives in patients with prior infarction but no acute ischemia. Coronary computed tomography angiography may identify the anatomical presence of stenosis²⁶ but cannot reveal a direct etiological link between chest pain and acute myocardial ischemia.

Physiological Basis for Ischemic Memory Imaging With Selectin Targeting

An imaging method that depicts a persisting physiological consequence of recent ischemia could establish a causal relationship between an episode of chest pain and acute myocardial ischemia. In the present study, we capitalized on the known sequence of inflammatory endothelial events occurring during myocardial ischemia-reperfusion and sought to detect them ultrasonically with acoustic markers capable of interrogating endothelial phenotype.^{11,12,19,27} Specifically, we imaged P-selectin, which, in the setting of coronary artery occlusion and reperfusion, is rapidly mobilized to the endothelial cell surface, where it mediates transient tethering interactions that slow leukocytes.^{7,28} The rapidity with which P-selectin is expressed after stimulation makes it an attractive marker when the question is

whether ischemia has recently occurred. Furthermore, its location on the endothelial cell surface renders it accessible to an intravascular probe such as a microbubble. Additionally, the major ligands for all 3 selectins are cell surface glycans possessing a specific sLe^x epitope,²⁹ meaning that a single moiety could be used to target both P- and E-selectins, which are expressed early and late, respectively, after reperfusion.

Ultrasound Ischemic Memory Imaging With Selectin-Targeted Microbubbles

We posited that a microbubble bearing sLe^x on its outer surface would enable detection and spatial localization of recent myocardial ischemia. We previously showed that an sLe^x-conjugated microbubble binds to activated cultured endothelial cells.¹³ In the present study, we took a stepwise approach to testing our hypothesis in vivo. First, we directly visualized microbubble-endothelial interactions using intravital microscopy of inflamed murine microcirculation. There was significantly greater adhesion of MB_{sLe^x} to inflamed vessels compared with noninflamed vessels. For inflamed mice, there was a trend toward greater adhesion of MB_{sLe^x} compared with MB_{CTL}. Similar to previous reports,¹⁵ there was slight nontargeted microbubble adhesion to inflamed microvasculature that, coupled with the relatively small sample sizes, accounted for the borderline statistical significance in the comparison between binding of MB_{sLe^x} and MB_{CTL} to inflamed endothelium.

Rats undergoing myocardial ischemia-reperfusion were then used to echocardiographically detect the adhesion events. Both early (30 minutes) and later (up to 90 minutes) after reflow, video intensity in the postischemic bed after injection of MB_{sLe^x} was significantly higher than that in the nonischemic bed. Additionally, within the same rat, video intensity within the ischemic zone after the injection of MB_{sLe^x} was higher than that after the injection of MB_{CTL}, indicating that the intravital microscopic observation of slight MB_{CTL} adhesion to inflammatory endothelium does not translate to nonspecific contrast enhancement during echocardiographic imaging.

Importantly, the region of persistent contrast enhancement colocalized with, and correlated in size to, the risk area. Furthermore, these findings could pertain to instances of milder (10 minutes) ischemia, in which we found a direction toward an increase in ischemic bed video intensity relative to that in the nonischemic bed after MB_{sLe^x} injection. Taken together, these data indicate that the selectin-targeted microbubbles were capable of “recalling” the presence, location, and spatial extent of previously ischemic myocardium.

The time frame during which ischemic memory imaging is possible with selectin as the target is incompletely characterized, although our data and the previous literature suggest a relatively extended window of opportunity. In murine intestinal microvasculature subjected to 20 minutes of ischemia, P-selectin more than doubled 10 minutes after reflow, increased further at 30 minutes, peaked at 5 hours, was still more than twice baseline at 8 hours, and returned to basal levels at 24 hours.³⁰ P-selectin immunohistochemical staining in feline myocardium peaked at 20 minutes after reperfusion (60% of venules), and at 130 minutes of reflow, 30% of venules still remained stained (versus 0% before reflow).³¹ In isolated rat hearts undergoing 60 minutes of ischemia, P-selectin was expressed on 80% of microvessels at 15 minutes of reflow and remained present on 36% of vessels after 60 minutes.³² Rat hearts subjected to 30 minutes of ischemia had significantly increased P-selectin on vascular

endothelium during a 2-hour reperfusion period.²⁰ Dogs undergoing transient myocardial ischemia and receiving an sLe^x bolus and 24-hour infusion had reduced infarct size and leukocyte accumulation compared with controls at 48 hours after reflow, whereas those receiving only bolused sLe^x did not derive protection, suggesting that physiologically significant P-selectin expression exists up to 48 hours after reperfusion.³³ This raises promise for the clinical utility of our selectin imaging during more extended reperfusion, although this needs to be systematically evaluated.

Comparison With Previous Studies

The present report is the first of myocardial ischemic memory imaging using ultrasound molecular targeting. A scintigraphic approach has used detection of suppressed fatty acid metabolism with the branched chain fatty acid β -methyl- ρ -[I¹²³]-iodophenyl-pentadecanoic acid.³⁴ The present study differs from the scintigraphic method in several obvious respects. First, we used ultrasound, which is advantageous in that it does not use radioisotopes, has a higher spatial resolution, and is a portable technique unencumbered by signal spillover from adjacent noncardiac tissue. Second, our molecular target was not intracellular but rather an endothelial surface epitope.

Non-ligand-targeted lipid microbubbles were used to detect postinfarction myocardial inflammation in canines via microbubble adhesion to activated leukocytes.¹⁹ Unlike that study, the animals in the present study had less infarction because our paradigm modeled the presentation of unstable angina in which myocyte necrosis is not the principal feature. Furthermore, we used specific ligand-directed adhesion directly to endothelium, rather than leukocyte tagging, as the targeting mechanism.

Study Limitations

MB_{sLe^x} could adhere to activated platelets expressing P-selectin,³⁵ possibly reducing bubble availability, but even if this occurred, detection of the postischemic region did not appear compromised. It is conceivable that MB_{sLe^x} bound both to endothelial P-selectin and platelets adherent to postischemic endothelium,³⁵ a phenomenon that could actually augment the acoustic signal.

To define the sensitivity of our method for detecting ischemic memory in the setting of time-dependent changes in adhesion molecule expression, the duration of diagnostically useful selectin imaging requires further characterization. This would necessitate additional studies using more elaborate chronic survival protocols than were possible in the present proof-of-concept study. On the basis of the present study and the literature cited above, the time window for diagnostically useful imaging could be several hours or perhaps longer, which would be ideal from the clinical implementation standpoint. In this regard, a multitargeted approach such as that previously described in vitro with sLe^x and anti-intercellular adhesion molecule-1 antibody¹³ also could be tested to further extend the time frame for imaging ischemic memory.

We modeled a situation in which ischemia duration would raise concern for an ACS but in which clinically obvious necrosis was not a major component. We chose 15 and 10 minutes

of occlusion because in rats there is extensive infarction beyond 15 minutes³⁶ and we deemed <10 minutes of ischemia as not representative of ACS. An inherent limitation of our model was that the goal of simulating ischemia without infarction was not consistently achieved; all but 6 rats had some necrosis by triphenyl tetrazolium chloride staining, albeit relatively limited. As such, what was actually imaged was P-selectin expression in mixed necrotic and viable tissue. Because the infarct was small, however, the preponderance of MB_{sLex} enhancement should be attributable to P-selectin expression in viable postischemic myocardium, so our claim of proof of ischemic memory imaging should still pertain.

The size of the 10-minute occlusion group precluded meaningful statistical analyses, but the mean data from this group are directionally consistent with the hypothesis that milder ischemia also generates ultrasonically detectable is-chemic memory. Nonetheless, results from this small sample should be viewed as exploratory and require further investigation. Additionally, milder degrees of ischemia resulting from various degrees of stenosis were not tested. Dreyer et al³⁷ showed in canines that even after milder degrees of myocardial ischemia in which flow reduction was only 31% to 50% of maximal flow during occlusion, there a 4-fold increase in endothelial neutrophil accumulation during reflow, consistent with significant endothelial activation even after mild ischemia.

Our approach is not specific to ischemia only but rather to inflammation. Other inflammatory processes causing chest pain such as myocarditis could cause targeted microbubble retention. Similarly, microvascular endothelial dysfunction associated with risk factors such as diabetes or hypercholesterolemia is a potential confounder if associated with selectin overexpression.³⁸ The images in these situations, however, would likely show spatially generalized contrast retention typical of a diffuse process,¹² whereas contrast enhancement resulting from ischemic memory would track discrete vascular territories.

Whether similar data are obtainable in patients with less favorable imaging windows remains to be determined. Higher transducer frequencies were required to image rat myocardium than typically used in humans, which may induce less nonlinear microbubble behavior because the natural harmonic frequency of microbubbles is lower.³⁹ Higher acoustic intensities resulting from more microbubble resonance at the lower transducer frequencies use in human imaging could compensate for the inherent limitations of acoustic windows in clinical populations. Ultimately, ultrasound systems designed specifically for molecular imaging applications are necessary to optimize the clinical detection of adhered microbubbles.

Clinical Implications

Ultrasonic identification of acute adhesion molecule expression on postischemic endothelium would enable not only the identification of recent myocardial ischemia but also the mapping of its location and spatial extent. The ability to causally link a discrete episode of chest pain to true myocardial ischemia would be a powerful clinical tool for the triage and subsequent testing of patients presenting with symptoms and clinical signs suggestive, but not diagnostic, of coronary ischemia. Further studies are required to determine the incremental value of this new approach to existing clinical diagnostic tools.

Acknowledgments

We gratefully acknowledge the statistical assistance provided by Thomas Kamarck, PhD, University of Pittsburgh.

Sources of Funding

This work was supported by RO1 HL58865 and HL077534 from the NHLBI (Dr Villanueva) and postdoctoral fellowship grants from the American Heart Association (Drs Lu and Pacella).

References

1. Burt CW. Summary statistics for acute cardiac ischemia and chest-pain visits to United States EDs, 1995–1996. *Am J Emerg Med.* 1999; 17:552–559. [PubMed: 10530533]
2. Lee TH, Rouan GW, Weisberg MC. Clinical characteristics and natural history of patients with acute myocardial infarction sent home from the emergency room. *Am J Cardiol.* 1987; 60:219–224. [PubMed: 3618483]
3. McCarthy BD, Beshansky JR, Selker HP. Missed diagnoses of acute myocardial infarction in the emergency department. *Ann Emerg Med.* 1993; 22:579–582. [PubMed: 8442548]
4. McCullough PA, Ayad O, Oneill WW, Goldstein JA. Costs and outcomes of patients admitted with chest pain and essentially normal electrocardiograms. *Clin Cardiol.* 1998; 21:22–26. [PubMed: 9474462]
5. Kosnik JW, Zalenski RJ, Shamsa F, Harris R, Mittner J, Kozlowski J, Di Carli M, Udelson JE. Resting sestamibi imaging for the prognosis of low-risk chest pain. *Acad Emerg Med.* 1999; 6:998–1004. [PubMed: 10530657]
6. Roberts RR, Zalenski RJ, Mensah EK, Rydman RJ, Ciavarella G, Gussow L, Das K, Kampe LM, Dickover B, McDermott MF, Hart A, Straus HE, Murphy DG, Rao R. Costs of an emergency department-based accelerated diagnostic protocol versus hospitalization in patients with chest pain: a randomized controlled trial. *JAMA.* 1997; 278:1670–1676. [PubMed: 9388086]
7. Krieglstein CF, Granger DN. Adhesion molecules and their role in vascular disease. *Am J Hypertens.* 2001; 14:44S–54S. [PubMed: 11411765]
8. Kurose I, Anderson DC, Miyasaka M, Tamatani T, Paulson JC, Todd RF, Rusche JR, Granger DN. Molecular determinants of reperfusion-induced leukocyte adhesion and vascular protein leakage. *Circ Res.* 1994; 74:336–343. [PubMed: 7507416]
9. Ley K, Bullard DC, Arbones ML, Bosse R, Vestweber D, Tedder TF, Beaudet AL. Sequential contribution of L and P selectin to leukocyte rolling in vivo. *J Exp Med.* 1995; 181:669–675. [PubMed: 7530761]
10. Weller GER, Villanueva FS, Klibanov AL, Wagner WR. Modulating targeted adhesion of an ultrasound contrast agent to dysfunctional endothelium. *Ann Biomed Eng.* 2002; 30:1012–1019. [PubMed: 12449762]
11. Weller GER, Wong MKK, Modzelewski RA, Lu E, Klibanov AL, Wagner WR, Villanueva FS. Ultrasonic imaging of tumor angiogenesis using contrast microbubbles targeted via the tumor-binding peptide RRL. *Cancer Res.* 2005; 65:533–539. [PubMed: 15695396]
12. Weller GER, Lu E, Csikari MM, Klibanov AL, Fischer D, Wagner WR, Villanueva FS. Ultrasound imaging of acute cardiac transplant rejection with microbubbles targeted to intercellular adhesion molecule-1. *Circulation.* 2003; 108:218–224. [PubMed: 12835214]
13. Weller GE, Villanueva FS, Tom EM, Wagner WR. Targeted ultrasound contrast agents: in vitro assessment of endothelial dysfunction and multi-targeting to ICAM-1 and sialyl Lewisx. *Biotechnol Bioeng.* 2005; 92:780–788. [PubMed: 16121392]
14. Bevilacqua MP, Nelson RM. Selectins. *J Clin Invest.* 1993; 91:379–387. [PubMed: 7679406]
15. Lindner JR, Song J, Xu F, Klibanov AL, Singbartl K, Ley K, Kaul S. Noninvasive ultrasound imaging of inflammation using microbubbles targeted to activated leukocytes. *Circulation.* 2000; 102:2745–2750. [PubMed: 11094042]
16. Lipowski HH, Zweifach BW. Application of the “two-slit” photometric technique to the measurement of microvascular volumetric flow rates. *Microvasc Res.* 1978; 15:93–101. [PubMed: 634160]

17. Reneman, RS.; Woldhuis, B.; oude Egbrink, MGA.; Slaaf, DW.; Tangelder, GJ. Concentration and velocity profiles of blood cells in the microcirculation. In: Hwang, NHC.; Turitto, VT.; Yen, MRT., editors. *Advances in Cardiovascular Engineering*. New York, NY: Plenum Press; 1992. p. 25-40.
18. Wei K, Jayaweera AR, Firoozan S, Linka A, Skyba DM, Kaul S. Quantification of myocardial blood flow with ultrasound-induced destruction of microbubbles administered as a constant venous infusion. *Circulation*. 1998; 97:473–483. [PubMed: 9490243]
19. Christiansen JP, Leong-Poi H, Klibanov AL, Kaul S, Lindner JR. Non-invasive imaging of myocardial reperfusion injury using leukocyte-targeted contrast echocardiography. *Circulation*. 2002; 105:1764–1767. [PubMed: 11956115]
20. Seko Y, Enokawa Y, Nakao T, Yagita H, Okumura K, Yazaki Y. Reduction of rat myocardial ischaemia/reperfusion injury by a synthetic selectin oligopeptide. *J Pathol*. 1996; 178:335–342. [PubMed: 8778341]
21. Lee TH, Cook EF, Weisberg MC, Sargent RK, Wilson C, Goldman L. Acute chest pain in the emergency room: identification and examination of low-risk patients. *Arch Intern Med*. 1985; 145:65–69. [PubMed: 3970650]
22. Zimmerman J, Fromm R, Meyer D, Boudreaux A, Wun CC, Smalling R, Davis B, Habib G, Roberts R. Diagnostic marker cooperative study for the diagnosis of myocardial infarction. *Circulation*. 1999; 99:1671–1677. [PubMed: 10190875]
23. Sabia P, Afrookteh A, Touchstone DA, Keller MW, Esquivel L, Kaul S. Value of regional wall motion abnormality in the emergency room diagnosis of acute myocardial infarction: a prospective study using two-dimensional echocardiography. *Circulation*. 1991; 84(suppl I):I-85–I-92. [PubMed: 1884510]
24. Rinkevich D, Kaul S, Wang XQ, Tong KL, Belcik T, Kalvaitis S, Lepper W, Dent JM, Wei K. Regional left ventricular perfusion and function in patients presenting to the emergency department with chest pain and no ST-segment elevation. *Eur Heart J*. 2005; 26:1606–1611. [PubMed: 15917277]
25. Udelson JE, Beshansky JR, Ballin DS, Feldman JA, Griffith JL, Heller GV, Hendel RC, Pope JH, Ruthazer R, Spiegler EJ, Woolard RH, Handler J, Selker HP. Myocardial perfusion imaging for evaluation and triage of patients with suspected acute cardiac ischemia: a randomized controlled trial. *JAMA*. 2002; 288:2693–2700. [PubMed: 12460092]
26. Achenbach S. Current and future status on cardiac computed tomography imaging for diagnosis and risk stratification. *J Nucl Cardiol*. 2005; 12:703–713. [PubMed: 16344233]
27. Leong-Poi H, Christiansen J, Klibanov AL, Kaul S, Lindner JR. Noninvasive assessment of angiogenesis by ultrasound and microbubbles targeted to alpha (v)-integrins. *Circulation*. 2003; 107:455–460. [PubMed: 12551871]
28. Lawrence MB, Springer TA. Leukocytes roll on a selectin at physiologic flow rates: distinction from and prerequisite for adhesion through integrin. *Cell*. 1991; 65:859–873. [PubMed: 1710173]
29. Foxall C, Watson SR, Dowbenko D, Fennie C, Lasky LA, Kiso M, Hasegawa A, Asa D, Brandley BK. The three members of the selectin receptor family recognize a common carbohydrate epitope, the sialyl Lewis (x) oligosaccharide. *J Cell Biol*. 1992; 117:895–902. [PubMed: 1374413]
30. Eppihimer MJ, Russell J, Anderson DC, Epstein CJ, Laroux S, Granger DN. Modulation of P-selectin expression in the post-ischemic intestinal microvasculature. *Am J Physiol*. 1997; 273:G1326–G1332. [PubMed: 9435558]
31. Weyrich AS, Buerke M, Albertine KH, Lefer AM. Time course of coronary vascular endothelial adhesion molecule expression during reperfusion of the ischemic feline myocardium. *J Leukoc Biol*. 1995; 57:45–55. [PubMed: 7530283]
32. Chukwemeka AO, Brown A, Venn GE, Chambers DJ. Changes in P selectin expression on cardiac microvessels in blood perfused rat hearts subjected to ischemia-reperfusion. *Ann Thorac Surg*. 2005; 79:204–211. [PubMed: 15620944]
33. Flynn DM, Buda AJ, Jeffords PR, Lefer DJ. A sialyl Lewisx-containing carbohydrate reduces infarct size: role of selectins in myocardial reperfusion injury. *Am J Physiol Heart Circ Physiol*. 1996; 40:H2086–H2096.

34. Dilsizian V, Bateman TM, Bergmann SR, Des Prez R, Magram MY, Goodbody AE, Babich JW, Udelson JE. Metabolic imaging with β -methyl- ρ -[^{123}I]-iodophenyl-pentadecanoic acid identifies ischemic memory after demand ischemia. *Circulation*. 2005; 112:2169–2174. [PubMed: 16186423]
35. Xu Y, Huo Y, Toufektsian MC, Ramos SI, Ma Y, Tejani AD, French BA, Yang Z. Activated platelets contribute importantly to myocardial reperfusion injury. *Am J Physiol Heart Circ Physiol*. 2006; 290:H692–H699. [PubMed: 16199480]
36. Tojo S, Yokota S, Koike H, Schultz J, Hamazume Y, Misugi E, Yamada K, Hayashi M, Paulson JC, Morooka S. Reduction in rat myocardial ischemia and reperfusion injury by sialyl Lewis x oligosaccharide and anti-rat P selectin antibodies. *Glycobiology*. 1996; 6:463–469. [PubMed: 8842711]
37. Dreyer WJ, Michael LH, West S, Smith CW, Rothlein R, Rossen RD, Anderson DC, Entman ML. Neutrophil accumulation in ischemic canine myocardium. *Circulation*. 1991; 84:400–411. [PubMed: 2060111]
38. Koh KK, Han SH, Quon MJ. Inflammatory markers and the metabolic syndrome: insights from therapeutic interventions. *J Am Coll Cardiol*. 2005; 46:1978–1985. [PubMed: 16325028]
39. de Jong N, Bouakaz A, Frinking P. Basic acoustic properties of micro-bubbles. *Echocardiography*. 2002; 19:229–240. [PubMed: 12022933]

CLINICAL PERSPECTIVE

Diagnosing acute coronary syndrome in patients presenting to the emergency room with chest pain is challenging. If symptoms have resolved or ECG changes are nondiagnostic, the diagnosis of acute or recent unstable myocardial ischemia can be difficult to make. Serum biomarkers of necrosis take time to become positive and may be negative in the presence of unstable angina unassociated with necrosis. Because recently ischemic endothelium acutely overexpresses P-selectin on its surface, this leukocyte adhesion molecule serves as the myocardial “memory” of a recent ischemic event. In the present study, an ultrasound contrast agent that binds specifically to P-selectin was developed and tested in rats undergoing experimental ischemia and reperfusion. After injection of the selectin-targeted agent during reperfusion, echocardiography demonstrated selective enhancement of the previously ischemic region, proving the concept that ultrasound ischemic memory imaging with P-selectin targeting can detect recent ischemia. If validated clinically, this 2-dimensional echocardiographic imaging approach targeting a specific molecular consequence of myocardial ischemia may facilitate the diagnosis of acute coronary syndrome.

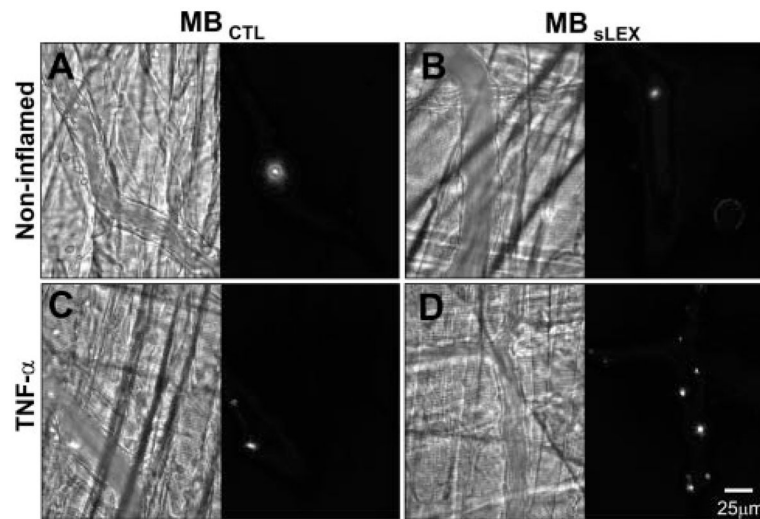


Figure 1. Photomicrographs of murine cremaster microcirculation under basal conditions (A, B) or tumor necrosis factor- α -induced inflammation (C, D) after intravenous fluorescent MB_{CTL} (A, C) or selectin-targeted MB_{sLEX} (B, D). Bright-field images are on the left and corresponding fluorescent images are on the right of each panel. There is greatest microbubble adhesion when MB_{sLEX} is injected into tumor necrosis factor- α -stimulated mice (D).

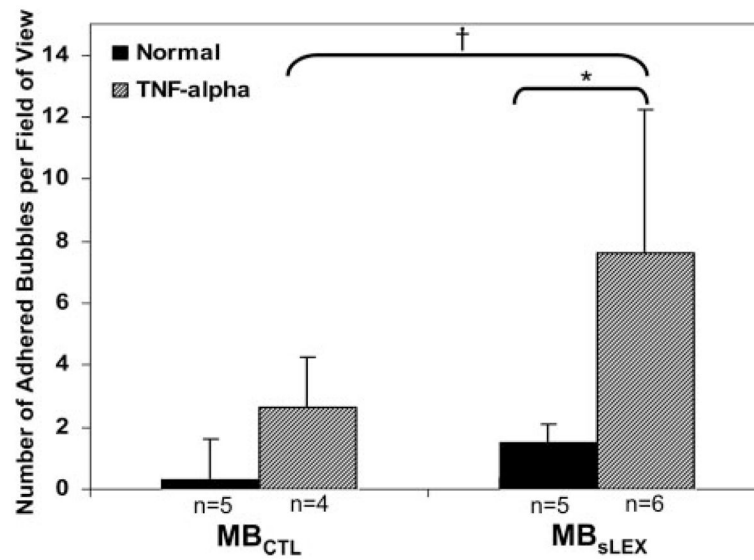


Figure 2. Extent of microbubble adhesion to murine cremaster microcirculation. There is greater MB_{sLEX} adhesion to tumor necrosis factor- α -stimulated microcirculation vs control tissue. Among tumor necrosis factor- α -stimulated mice, there was a strong trend toward greater adhesion of MB_{sLEX} vs MB_{CTL}. * $P=0.0081$; † $P=0.07$.

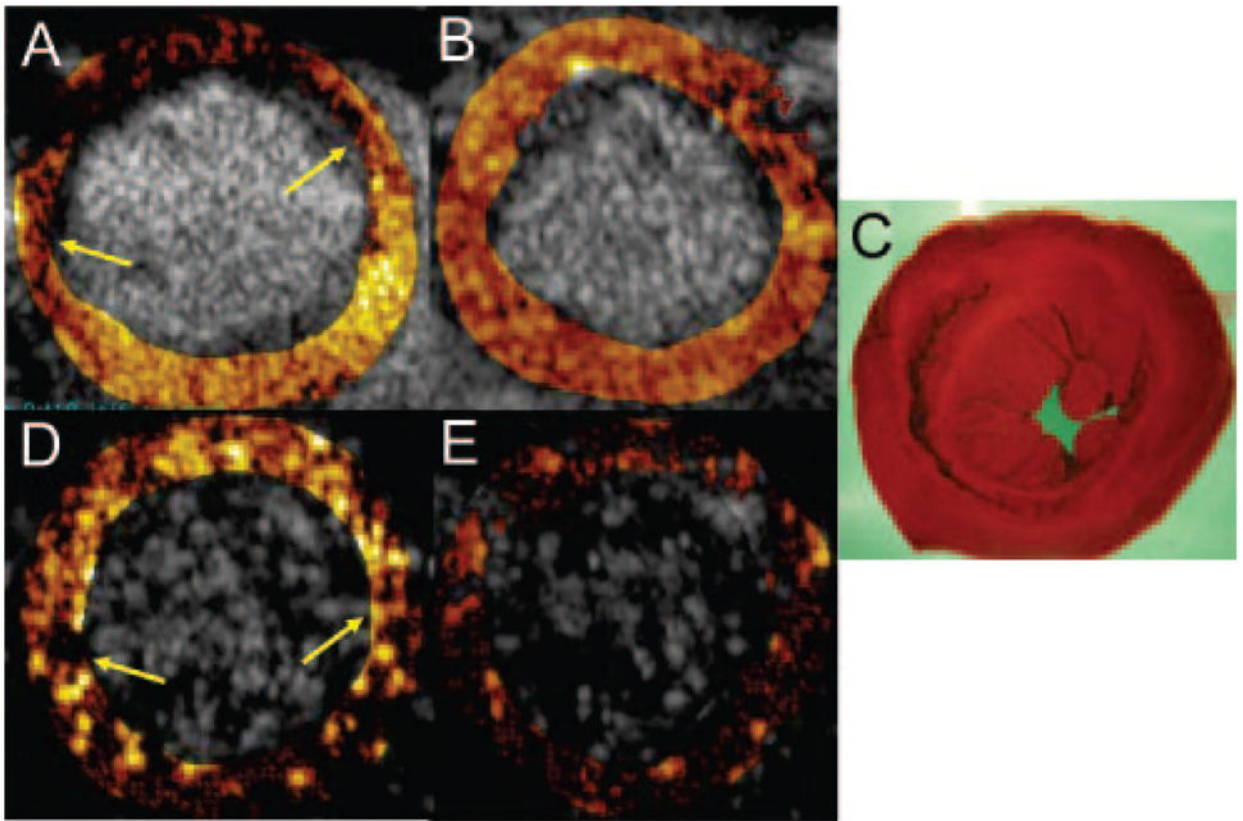


Figure 3. Ischemic memory imaging at 30 minutes after reflow in 1 rat undergoing 15 minutes of ischemia but sustaining no infarction (C). The myocardial contrast echocardiograms are represented as subtraction images, with values for contrast change color-coded for each pixel. The risk area during occlusion (contrast-deficient region between arrows in A) resolves after reperfusion (B). For the MCE images in D and E, the image at 4 minutes after contrast injection has been subtracted from the 3.5-minute image to yield the signals attributable to adhesion. After injection of sLe^x-conjugated microbubbles, there is persistent contrast enhancement (region between arrows in D) within the previously ischemic area (A), which is not seen after injection of control microbubbles (E).

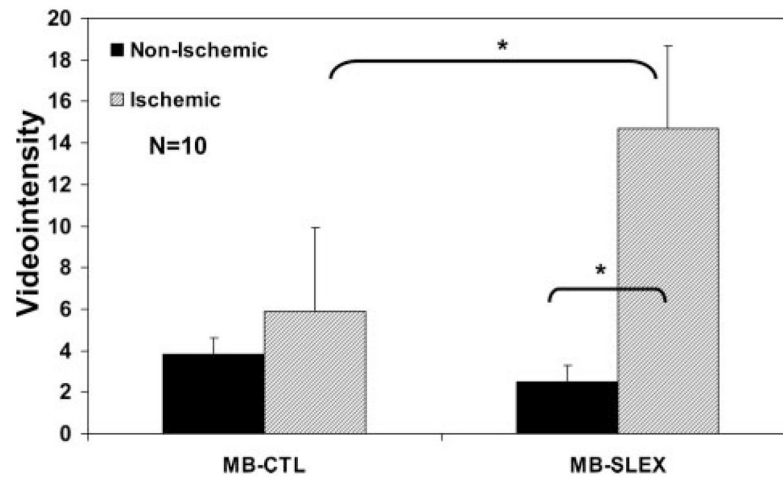


Figure 4. Video intensity measurements in the postischemic and nonischemic regions at 30 minutes after reflow in rats undergoing 15 minutes of coronary occlusion after injection of control microbubbles (MB-CTL) or selectin-targeted microbubbles (MB-SLEX) in each rat. * $P=0.002$.

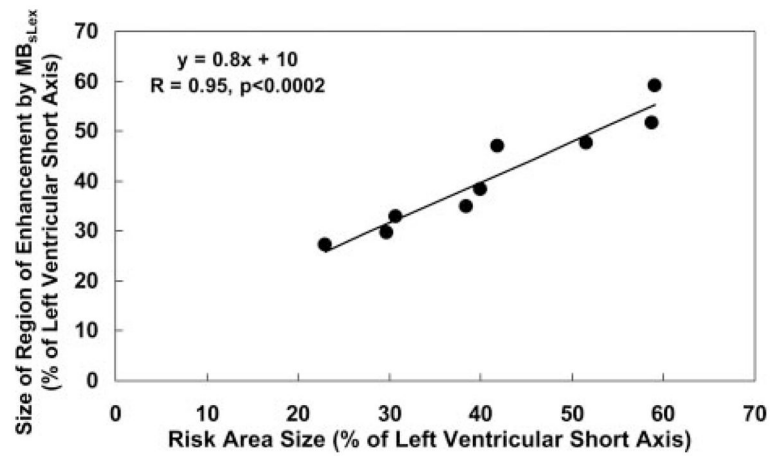


Figure 5.

Linear relationship between the size of the risk area and the size of the region of contrast enhancement after MB_{sLex} injection at 30 minutes of reflow in rats undergoing 15 minutes of occlusion. Antemortem risk area measurement could not be obtained in 1 of the 10 rats in this group. Measurements are expressed as a percent of the short-axis slice of the left ventricle.

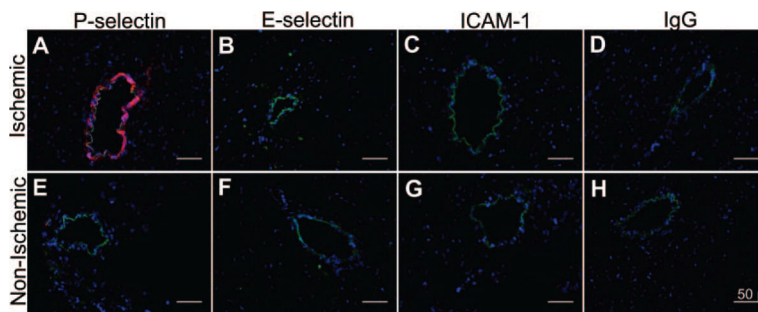


Figure 6.

Fluorescent immunohistochemical staining of postischemic (A–D) and nonischemic (E–H) myocardium 45 minutes after reperfusion. Nuclei are stained blue (Hoechst stain); endothelium is stained green (fluorescein-labeled secondary antibody against anti-CD31 primary antibody). Rhodamine-labeled secondary antibodies (red) are directed against primary antibodies to P-selectin (A, E), E-selectin (B, F), intercellular adhesion molecule-1 (C, G), and nonspecific immunoglobulin G (D, H). Endothelial P-selectin is present in postischemic microvasculature only (A). The other adhesion molecules are not acutely expressed.